Friction **11**(3): 395–409 (2023)
https://doi.org/10.1007/s40544-022-0604-y
ISSN 2223-7690
CN 10-1237/TH
RESEARCH ARTICLE

Carbon fiber cannot always reduce the wear of PEEK for orthopedic implants under DPPC lubrication

Shuai YAN*, Shichao MEN, Hongbo ZOU, Haoji WANG, Zhongjiang ZHANG, Chunshen WANG, Tianyi SUI, Bin LIN*
Key Laboratory of Advanced Ceramics and Machining Technology of Ministry of Education, Tianjin University, Tianjin 300072, China
Received: 21 October 2021 / Revised: 28 November 2021 / Accepted: 29 January 2022

Abstract: Excellent wear resistance is an important feature of orthopedic implants. However, although pure polyetheretherketone (PEEK) is outperformed by carbon fiber-reinforced PEEK (CF-PEEK) for stability and durability under laboratory conditions, it is not clear whether CF-PEEK should be preferred in all real-world applications. Results indicate that, under dipalmitoylphosphatidylcholine (DPPC) lubrication, the wear rates of PEEK are 35%–80% lower than the wear rates of CF-PEEK for different implant materials, speeds, loadings, and DPPC concentrations. Molecular dynamics calculations confirm that DPPC self-assembles on the PEEK surface to form an easily adsorbed continuous phospholipid lubricating film. In contrast, the carbon fibers on the CF-PEEK surface hinder the formation of the protective DPPC film and the CF-PEEK surface is thus subject to faster wear.

Keywords: polyetheretherketone (PEEK); carbon fiber-reinforced PEEK (CF-PEEK); dipalmitoylphosphatidylcholine (DPPC); orthopedic implants; self-assembly

1 Introduction

Polyetheretherketone (PEEK) is a fully aromatic, semicrystalline thermoplastic with high wear resistance, rigidity, strength, thermal stability, chemical resistance, and radiation damage resistance. PEEK and enhanced PEEK are widely used in the manufacture of aircraft parts and other equipment used under extreme conditions [1–3]. In the field of orthopedic implants, PEEK is a high-wear-resistance orthopedic biomaterial with an elastic modulus close to that of human cortical bone, good biocompatibility, and high transmittance [4–6]. Recently, PEEK has been successfully applied in spinal interbody fusion and other orthopedic applications. Given its excellent wear resistance, PEEK has thus attracted considerable attention as an implant material [7–9] and possible replacement for polyethylene polymer implant materials [10]. For example, Brockett et al. [5] found that PEEK reduced the wear rate by 60% compared to ultrahigh-molecular-weight polyethylene (UHMWPE).

In contrast, carbon fiber-reinforced PEEK (CF-PEEK) has demonstrated even better mechanical properties and stability than pure PEEK, while maintaining good biocompatibility. In particular, numerous preliminary orthopedic implant studies indicate that the wear resistance of CF-PEEK is superior to that of PEEK under laboratory conditions [11–13]. For example, in the early 1990s, Maharaj et al. [14] experimentally determined the tribological properties of CF-PEEK and ZrO_2 under bovine serum and water lubrication and found that the wear rate of CF-PEEK was only one tenth that of UHMWPE. Later, Wang et al. [15] explored the applicability of medical-grade CF-PEEK and UHMWPE as load-bearing surfaces in total hip arthroplasty; they found that the wear rate of the CF-PEEK articulating against Al_2O_3, ZrO_2, and CoCr under bovine serum lubrication was lower than that of the UHMWPE friction pair. Given these highly promising results, it is unsurprising that CF-PEEK is widely considered to be an ideal polymer material for the next generation of orthopedic implants.

* Corresponding authors: Shuai YAN, E-mail: yanshuai@tju.edu.cn; Bin LIN, E-mail: linbin@tju.edu.cn

Parallel breakthrough discoveries are also being made in the lubrication materials that facilitate the high-performance operation of these artificial implants. In the process of friction and lubrication within natural joints, the cartilage covering the joint surfaces and the synovial fluid in the joint play vital roles. In a healthy joint, the cartilage tissue effectively prevents direct contact between joint materials, greatly reducing wear [16]. In artificial joints, the lubricants between the friction surfaces mainly include deionized water, calf serum, and sodium hyaluronate [17–19]. In recent years, phosphatidylcholine liposomes have emerged as high-quality biomimetic joint lubricants and biomimetic articular cartilage materials [20–23]. Therefore, it is important to study the tribological properties of artificial joint friction pairs under phospholipid lubrication. Common phospholipids include 1,2-dipalmitoyl-sn-glycero-3-phosphocholine (DPPC), 1,2-dimyristoyl-snglycero-3-phosphocholine (DMPC), 1,2-dilauroyl-sn-glycero-3-phosphocholine (DLPC), 1,2-distearoyl-sn-glycero-3-phosphocholine (DSPC), and 1-palmitoyl-2-stearoyl-sn-glycero-3-phosphocholine (HSPC). Especially, DPPC has been successfully used as a drug carrier for treating human organ diseases [24, 25]. Therefore, DPPC has great potential as the first high-efficiency lubricant injected into human joints [26, 27]. In 2016, Sorkin et al. [28] investigated the hydration lubrication of lipid bilayer boundary lubricants in dipalmitoyl phosphatidylcholine (DPPC) dispersions and reported self-healing induced by phosphatidylcholine shearing. Four years later, Angayarkanni et al. [29] studied the lubrication of phospholipids at the boundaries of artificial joints and observed that phospholipids self-assemble during the lubrication process. These two phenomena (self-assembly and self-healing) allow the phospholipids to continuously provide ultra-low friction and ultra-small wear during the lubrication process.

These dramatic improvements in the artificial synovial fluid replacement materials have been further matched by ceramic materials discoveries. Ceramic artificial joint materials such as silicon nitride (Si_3N_4), alumina (Al_2O_3), and zirconia (ZrO_2) have attracted considerable research attention in recent years. Compared to metals, these ceramic materials have very low friction coefficients, very low wear rates, and excellent biological compatibility [30–33]. In recent studies, ceramic materials and PEEK have been combined to form new friction pairs. For example, in studying the performance of biocompatible Si_3N_4 and PEEK in a DPPC lubrication condition, Wang et al. [34] found that the friction coefficient between PEEK and Si_3N_4 reached 0.04. However, no comparative study with CF-PEEK and DPPC was conducted.

To better evaluate the combination of next-generation high-performance artificial implant materials, the present study determined whether or not carbon fibers can reduce the wear rate of PEEK articulating against ceramics under DPPC lubrication. The wear rates of PEEK and CF-PEEK articulating against ceramics under DPPC lubrication were systematically studied at different friction speeds and loads, and the friction mechanisms of PEEK and CF-PEEK under DPPC lubrication were analyzed.

2 Materials and methods

2.1 Materials

Medical-grade PEEK and CF-PEEK were obtained from the Invibio Company (UK) and their respective physical parameters are shown in Table 1. CF-PEEK with randomly distributed carbon fibers was selected to prevent the influence of carbon fiber orientations. CF-PEEK contains 30% weight fraction of pitch-based carbon fibers and the length of these carbon fibers is 25 μm [35]. Commercial balls of four different materials commonly used to mimic bone in artificial implants were obtained from the China National Machinery Industry Corporation, (China): Si_3N_4, Al_2O_3, ZrO_2, and stainless steel. The diameter of all balls was 9.525 mm and their physical parameters are shown in Table 2. DPPC 16:0 (Mw = 734.04 g·mol^{-1}, purity ≥ 99%) was obtained from Macklin Biochemical Technology Co., Ltd. (Shanghai, China). The main transformation temperature (T_m) of the DPPC is 41.6 °C [34].

In the experiment, 10 g/L DPPC aqueous solution was prepared according to standard approaches presented in the literature [36–39]. All experimental processes were carried out at temperatures above the main phase transition temperature ($T > T_m$) of DPPC. DPPC was hydrated with deionized water and subjected to ultrasonic processing (JP-010-t, SKYMEN, China) for 1,800 s to obtain 10 g/L DPPC aqueous

Table 1 Physical parameters of PEEK.

Material	PEEK	CF-PEEK
Model	PEEK-OPTIMA® Natural	PEEK-OPTIMA® Wear performance
Density (g/cm^3)	1.30	1.43
Flexural modulus (GPa)	4.0	6.3
Poisson's ratio	0.36	0.41
Compressive strength (MPa)	135	200
Roughness Ra (μm)	0.05	0.05

Table 2 Physical parameters of the different experimental materials.

Material	Si_3N_4	Al_2O_3	ZrO_2	Stainless steel
Young's modulus (GPa)	310	380	210	200
Poisson's ratio	0.26	0.22	0.30	0.30
Roughness Ra (μm)	0.01	0.01	0.01	0.01

solution. The DPPC aqueous solution was diluted to 1 g/L and stirred with a magnetic heated stirrer (JK-DMS-H, SKI, China) for 7,200 s. The 1 g/L DPPC aqueous solution maintained a homogeneous hydration state.

2.2 Methods

2.2.1 *Friction experiments*

Friction reciprocating tests were carried out using a ball-on-disc tribological testing machine (UMT-TriboLab, Bruker, USA). Before tribological testing, all samples were subjected to ultrasonic treatment with alcohol and pure water to ensure accurate experimental data. The tribological testing temperature was 22±3 °C. The loads applied in the friction experiment were 5, 10, and 15 N (Hertz stress = 90–200 MPa). The tribological test time was 3,600 s. These loads are in line with the Hertz stress limit required for human joints [34, 40] and these loads meet the compressive strength of all materials. The reciprocating frequencies were 1, 1.5, and 2 Hz (sliding speed = 20–40 mm·s^{-1}). Figure 1 depicts the experimental friction process.

2.2.2 *Characterization and test methods*

The friction coefficients of the different experimental materials were recorded and output by a UMT-TriboLab tribological properties testing machine in real time. A non-contact profilometer (ST400, Nanovea Ltd., USA) was used to measure the wear scars on the PEEK discs. Wear rate (w) of the PEEK and CF-PEEK discs was determined by Eq. (1) (according to the ASTM-G99 Standard [41]):

$$w = \frac{V_d}{D \cdot F} \tag{1}$$

where V_d (mm^3) is volume of the worn track. D (m) and F (N) stand for sliding distance and normal load, respectively.

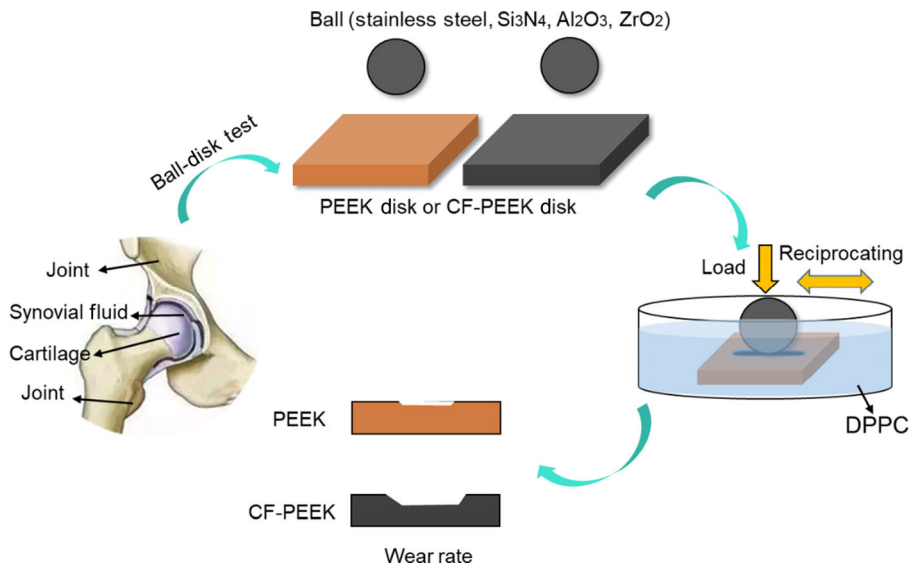

Fig. 1 Experimental friction method and process.

$$V_d = l \cdot \left(\frac{S_1 + S_2 + S_3}{3} \right) \quad (2)$$

where S_n (n = 1, 2, 3) is cross-section area of the worn track, which got directly from non-contact profilometer (ST400, Nanovea Ltd., USA). l stands for the length of scratch (l = 10 mm).

After the friction experiment, the friction scratches, friction surface film, and wear interface on the PEEK disc were observed with a super-depth-of-field microscope (VHX-7000, KEYENCE, Japan). X-ray photoelectron spectroscopy (XPS; ESCALAB Xi+, Thermo Fisher, USA) was used to study the film in the friction scratches of the PEEK disc. The morphology and film thickness in the PEEK disc scratches were evaluated by atomic force microscopy (AFM; Dimension Icon, Bruker, Germany).

3 Results

3.1 Tribological behaviors of different materials

Figure 2 shows the average friction coefficients (Fig. 2(a)) and wear rates (Fig. 2(b)) of PEEK and CF-PEEK with stainless steel, Si_3N_4, Al_2O_3, and ZrO_2, under water lubrication. It is clear that, in each case, CF-PEEK had a dramatically lower friction coefficient and a commensurately lower wear rate under water lubrication. For example, the wear rate of the PEEK/stainless steel friction pair was 21.5×10^{-6} mm^3/(N·m), while that of the CF-PEEK/stainless steel pair was only 2.2×10^{-6} mm^3/(N·m) (i.e., the wear rate of CF-PEEK was only 10% that of PEEK).

Figure 2 also shows the average friction coefficients (Fig. 2(c)) and wear rates (Fig. 2(d)) of PEEK and CF-PEEK under DPPC lubrication. PEEK and CF-PEEK showed similar friction coefficients under DPPC lubrication, as shown in Fig. 2(c). Nevertheless, the friction coefficient was lowest between Si_3N_4 and PEEK (a reduction of 67% compared to water lubrication), which indicates that Si_3N_4 may be preferable for use in artificial joints with DPPC lubrication [31, 42]. Surprisingly, the wear rate of the PEEK/Si_3N_4 friction pair was 0.3×10^{-6} mm^3/(N·m), which is only 21% of the wear rate of the CF-PEEK/Si_3N_4 friction pair (1.4×10^{-6} mm^3/(N·m)). In sum, CF-PEEK dramatically outperforms PEEK under water lubrication, but PEEK dramatically outperforms CF-PEEK under DPPC lubrication.

The fact that the wear rate of CF-PEEK is strongly dependent on the type of lubricant contradicts the current predictions that CF-PEEK will outperform PEEK in biomedical applications [43, 44]. Given the advantages of using DPPC-related phospholipids in

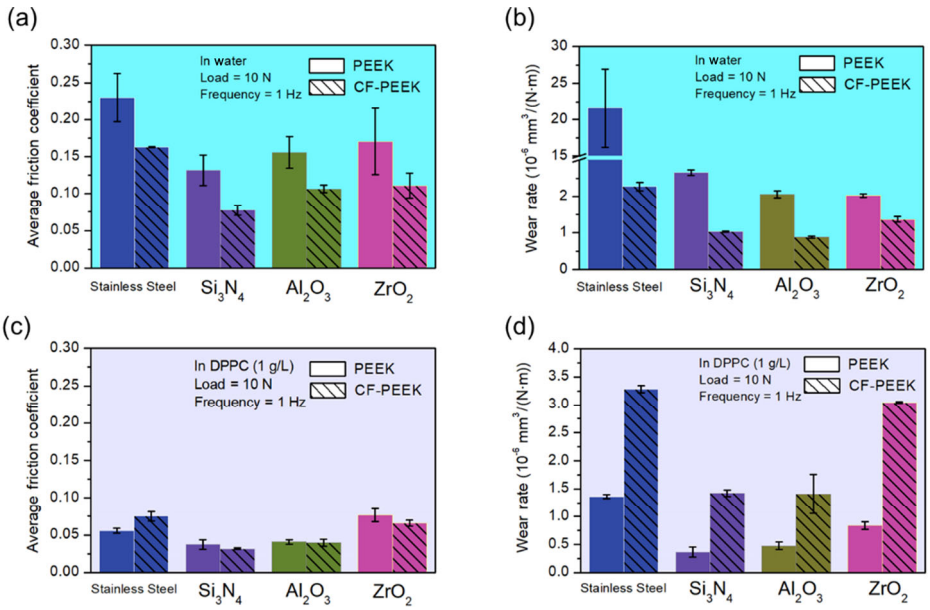

Fig. 2 Average friction coefficients and wear rates of PEEK and CF-PEEK under water and DPPC (1 g/L) lubrication. (a) Average friction coefficients under water lubrication; (b) average wear rates under water lubrication; (c) average friction coefficients under DPPC (1 g/L) lubrication; and (d) average wear rates under DPPC (1 g/L) lubrication.

biomimetic cartilage and biomimetic joint lubricants [27, 38, 45], it is therefore necessary to understand the tribological properties of artificial implant materials under DPPC lubrication. Because the wear rates were lowest for the PEEK/Si_3N_4 and CF-PEEK/Si_3N_4 friction pairs under DPPC lubrication. Hence, we systematically studied the tribological properties and tribological mechanism of PEEK/Si_3N_4 and CF-PEEK/Si_3N_4 under DPPC lubrication.

3.2 Tribological behaviors of PEEK and Si_3N_4

We systematically changed the experimental load and speed to study the tribological properties of the PEEK/Si_3N_4 and CF-PEEK/Si_3N_4 pairs under water

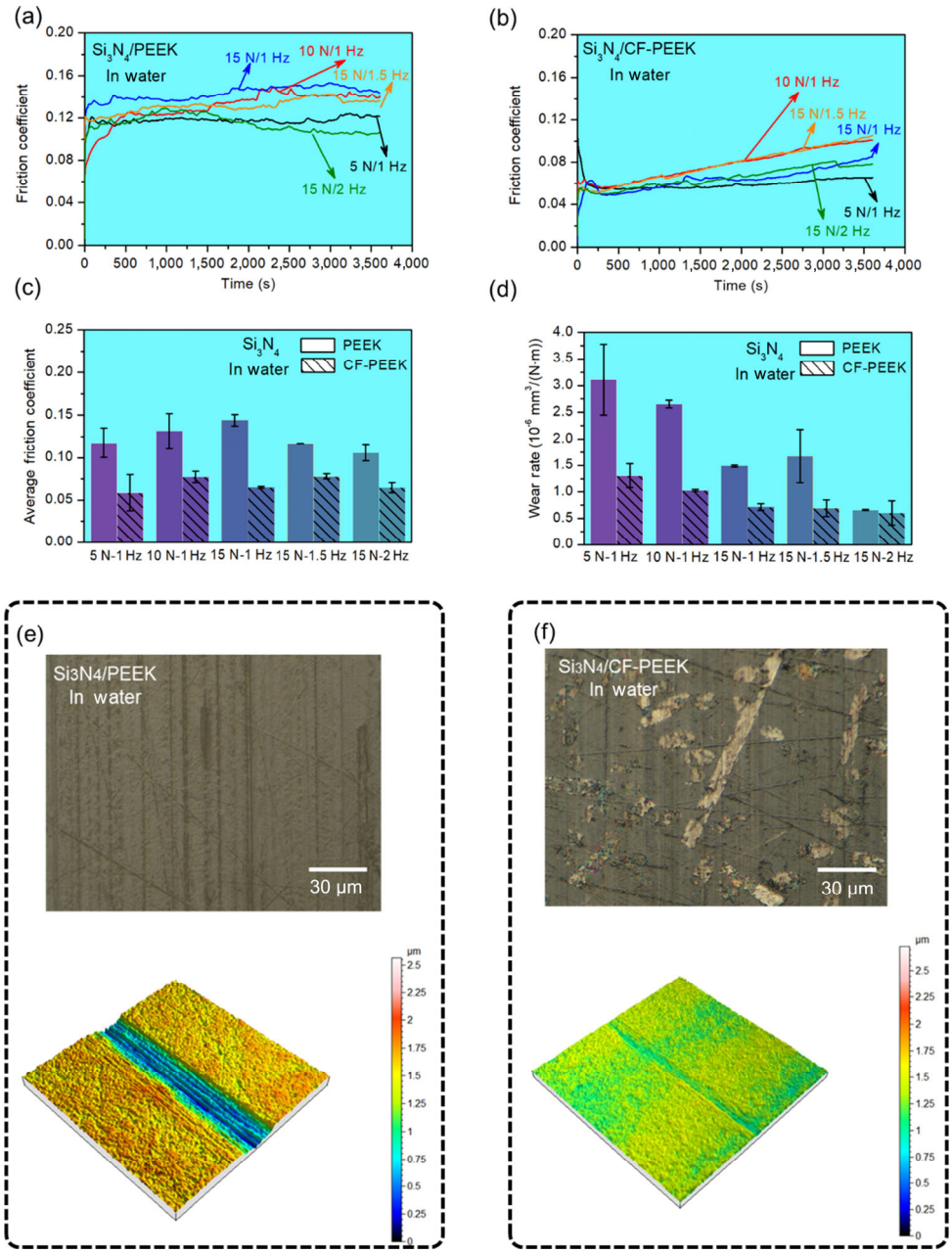

Fig. 3 Friction coefficients and wear rates of PEEK and CF-PEEK for all experimental conditions (5 N-1 Hz, 10 N-1 Hz, 15 N-1 Hz, 15 N-1.5 Hz, and 15 N-2 Hz) under water lubrication. (a) Friction coefficients of PEEK in water; (b) friction coefficients of CF-PEEK in water; (c) average friction coefficients of PEEK and CF-PEEK in water; (d) wear rates of PEEK and CF-PEEK in water; (e) microscopic morphology and 3D morphology of PEEK after tribological testing in water; and (f) microscopic morphology and 3D morphology of CF-PEEK after tribological testing in water.

lubrication. Figure 3 shows the PEEK/Si_3N_4 friction coefficients (Fig. 3(a)) and wear rates (Fig. 3(d)) in comparison with the CF-PEEK/Si_3N_4 friction coefficients (Fig. 3(b)) and wear rates (Fig. 3(d)) during the friction process under water lubrication. As anticipated, CF-PEEK showed a much lower average friction coefficient (Fig. 3(c)) and wear rate (Fig. 3(d)) for all experimental conditions (5 N-1 Hz, 10 N-1 Hz, 15 N-1 Hz, 15 N-1.5 Hz, and 15 N-2 Hz). Microscopy and three-dimensional (3D) morphological scanning were then applied to observe the surfaces of PEEK (Fig. 3(e)) and CF-PEEK (Fig. 3(f)), visually confirming that the pits on the surface of the CF-PEEK were shallower than those on the surface of the PEEK.

As our initial experiment indicated, the tribological properties of the PEEK/Si_3N_4 and CF-PEEK/Si_3N_4 pairs were dramatically different under DPPC lubrication (1 g/L). Figure 4 shows the PEEK/Si_3N_4 friction

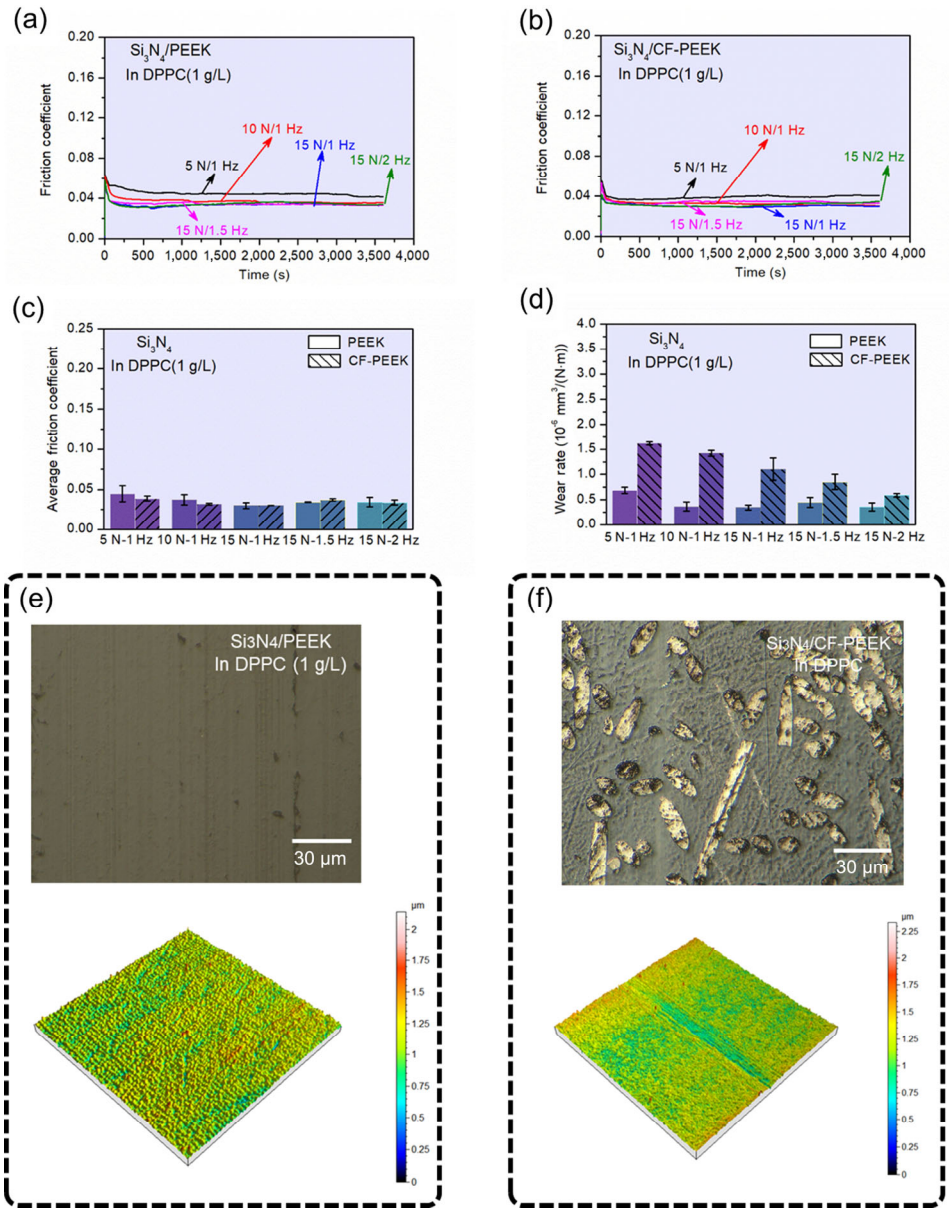

Fig. 4 Friction coefficients and wear rates of the PEEK/Si_3N_4 and CF-PEEK/Si_3N_4 friction pairs under DPPC (1 g/L) lubrication and different experimental conditions (5 N-1 Hz, 10 N-1 Hz, 15 N-1 Hz, 15 N-1.5 Hz, and 15 N-2 Hz). (a) Friction coefficients of PEEK in DPPC; (b) friction coefficients of CF-PEEK in DPPC; (c) average friction coefficients of PEEK and CF-PEEK in DPPC; (d) wear rates of PEEK and CF-PEEK in DPPC; (e) microscopic morphology and 3D morphology of PEEK after tribological testing in DPPC; and (f) microscopic morphology and 3D morphology of CF-PEEK after tribological testing in DPPC.

coefficients (Fig. 4(a)) and wear rates (Fig. 4(d)) in comparison with the CF-PEEK/Si_3N_4 friction coefficients (Fig. 4(b)) and wear rates (Fig. 4(d)) during the friction process under DPPC lubrication. For all experimental conditions (5 N-1 Hz, 10 N-1 Hz, 15 N-1 Hz, 15 N-1.5 Hz, and 15 N-2 Hz), the friction coefficients of the PEEK/Si_3N_4 and CF-PEEK/Si_3N_4 pairs remained in the range of 0.03–0.05. However, despite their very similar, low, and stable friction coefficients, the wear rates of PEEK are consistently 50%–75% lower than the wear rates of CF-PEEK (Fig. 4(d)). To understand this phenomenon, we used a microscope to observe the worn and cleaned surfaces of PEEK and CF-PEEK under the experimental condition of 10 N-1 Hz in DPPC (1 g/L), where the contrast was most dramatic (Figs. 4(e) and 4(f)). In sum, although DPPC shows great potential as a new biomimetic articular fluid and biomimetic articular cartilage material to reduce the wear of artificial bone materials [40], CF-PEEK may have significantly lower wear resistance than ordinary PEEK in DPPC.

4 Discussion

4.1 Material characterization analysis

To more clearly understand the effect of carbon fiber on wear, the wear efficiency was calculated using the Eq. (3) [46]:

$$\text{Efficiency}=\frac{\text{Wear}_{\text{PEEK}}-\text{Wear}_{\text{CF-PEEK}}}{\text{Wear}_{\text{PEEK}}} \tag{3}$$

An efficiency greater than zero means that carbon fiber reduces wear (CF-PEEK outperforms pure PEEK), while an efficiency less than zero means that carbon fiber increases wear (pure PEEK outperforms CF-PEEK). The wear efficiencies obtained in this study are compared with previously reported values in Fig. 5.

Zhu et al. [47] reported that CF-PEEK has a wear rate 40% lower than PEEK's under dry friction. Wang et al. [48] found that varying the carbon fiber in CF-PEEK could reduce the wear rate of PEEK by as

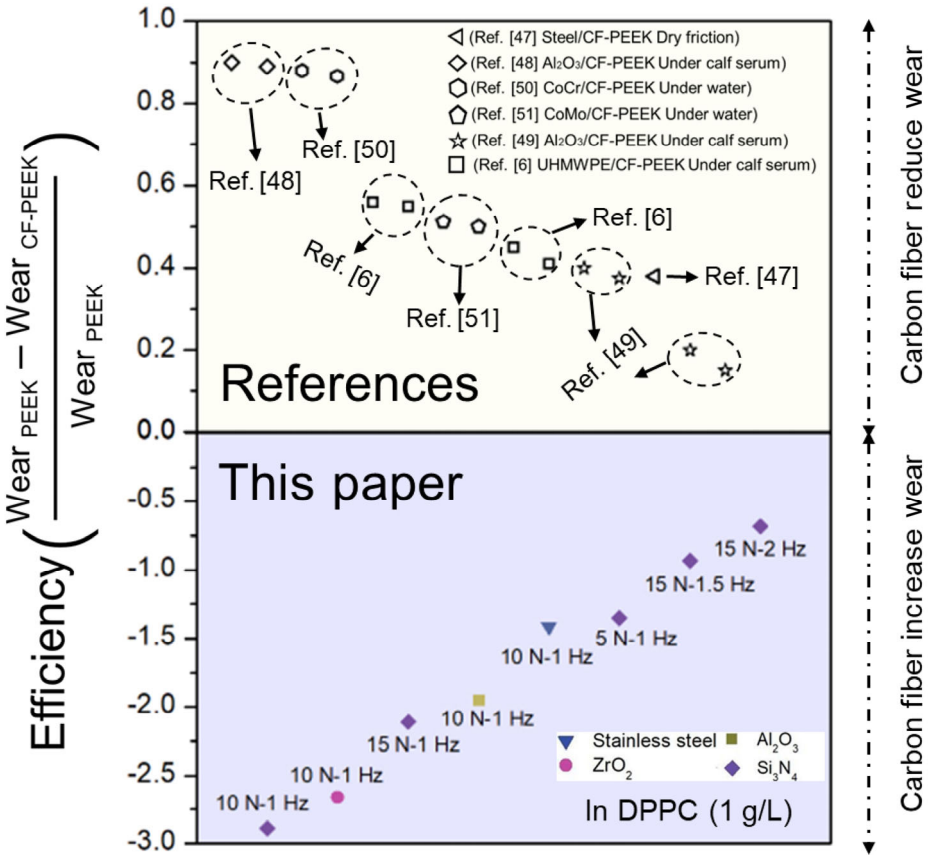

Fig. 5 Comparison of CF-PEEK wear efficiencies obtained in this study with those reported elsewhere.

much as 90% under calf serum lubrication. Regis et al. [49] found that CF-PEEK maintained its excellent wear resistance under calf serum lubrication. Under water or human serum lubrication, Borruto [50] found that CF-PEEK had a wear rate approximately 80% lower than pure PEEK. Yamamoto and Hashimoto [51] similarly reported that CF-PEEK reduced the wear rate of PEEK by 50% under water lubrication. Song et al. [6] found that the wear rate of CF-PEEK was only half that of PEEK under calf serum lubrication. The reason why carbon fiber reduces PEEK wear rate inconsistently in the above references may be under a variety of conditions, with different materials and lubrications, and even different ratios of carbon fibers. In stark contrast, the present study suggests that, under DPPC lubrication specifically, the wear efficiency was less than zero (Fig. 5).

Figure 6(a) shows a microscopy image of the scratches on the PEEK surface after tribological testing under 1g/L DPPC lubrication, where DPPC clusters adsorbed on the PEEK surface then combined into a continuous large lubricating film [38, 52, 53], which is known to

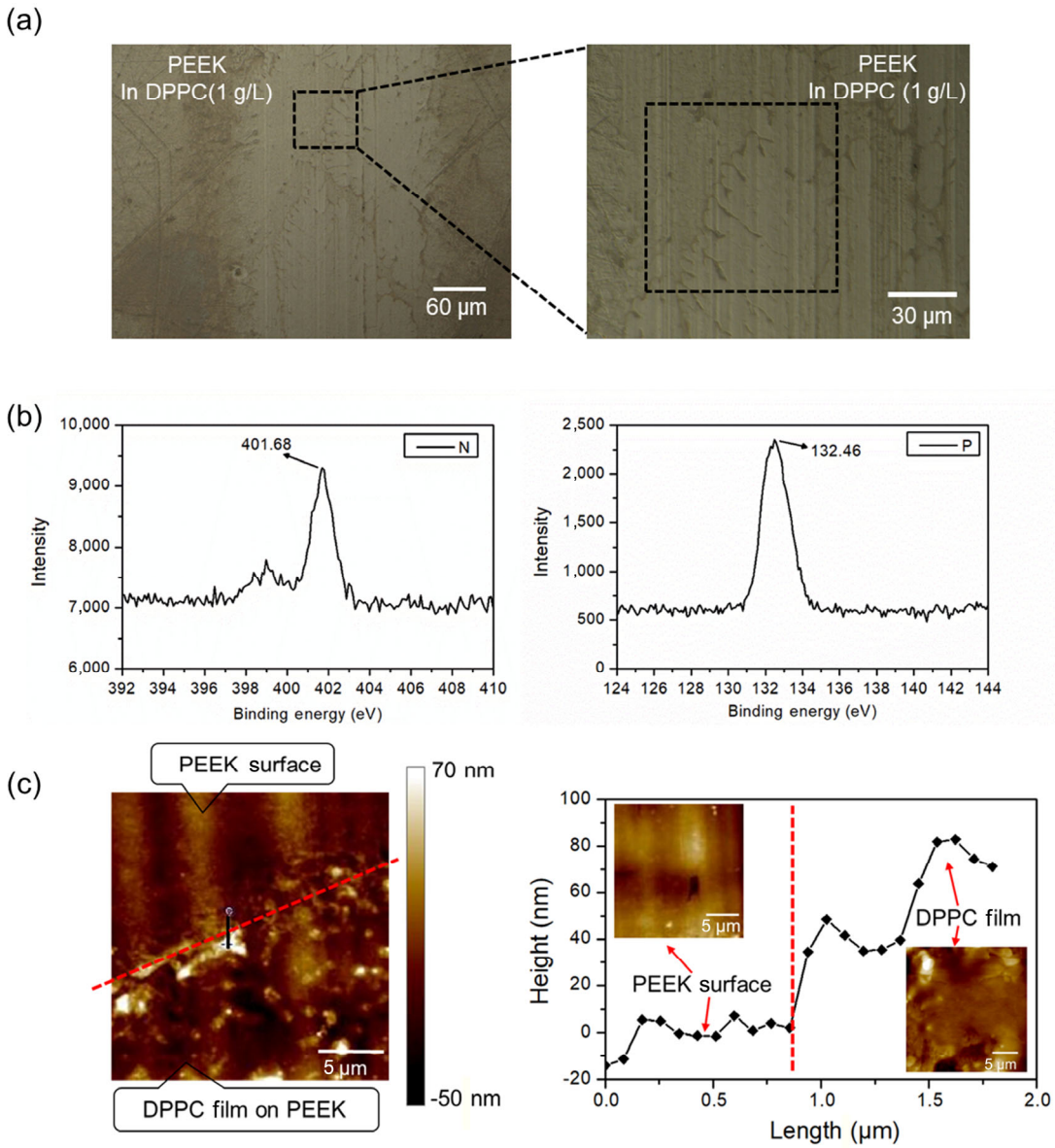

Fig. 6 Analysis of the DPPC film on the PEEK surface after tribological testing in 1 g/L DPPC. (a) Microscopy images showing the surface morphology of PEEK in DPPC (1 g/L); (b) XPS spectra of the PEEK surface film; and (c) AFM analysis of the PEEK surface film.

play an important role in lubrication and friction reduction on the PEEK surface [45, 54]. The inset 30 μm image shows that large, continuous lubricating films covered the scratches on the PEEK surface. In the XPS spectra of the surface film (Fig. 6(b)), N 1s and P 2p peaks are clearly observed, confirming that the film on the surface of PEEK was a DPPC phospholipid film [34]. The height difference between the PEEK surface and the DPPC-coated PEEK surface can be clearly observed (Fig. 6(c)), further confirming that DPPC was continuously adsorbed on the PEEK surface during the tribological testing of the PEEK/Si_3N_4 friction pairs. This process can be described as the self-assembly of the DPPC film [28, 29, 55], and was previously demonstrated by Klein's group on the atomic scale [26, 28, 29, 56]. Our research group has clearly shown that the self-assembly of DPPC affects the tribological properties of PEEK on the macroscale [28, 29].

To better understand the anomalous results for CF-PEEK in a DPPC concentration, we conducted the friction experiment of CF-PEEK/Si_3N_4 (10 N-1 Hz) under 1 g/L DPPC concentration (Fig. 7). Rather than forming a continuous film, DPPC formed small, irregular pieces on a relatively small percentage of the CF-PEEK surface. Rather than self-assembling [28, 29], the carbon fiber matrix inhibited the formation of a continuous bulk DPPC phospholipid on the CF-PEEK surface. Because the DPPC was unable to establish a large positive pressure-bearing capacity, the CF-PEEK achieved relatively poor tribological properties and a much higher wear rate.

To better understand the role that DPPC plays in lubrication, and how the amount of DPPC impacts the reduction in PEEK wear, we first calculated he wear rates of pure PEEK/Si_3N_4 (10 N-1 Hz) under different DPPC concentrations (0.1, 0.2, 0.5, 1.0, and 2.0 g/L) (Fig. 8). The wear rate of PEEK at a DPPC concentration of 0.1 g/L was like that under water lubrication. However, when the DPPC concentration exceeded 0.2 g/L, DPPC began to play a lubricating role in the friction process. We speculate that when the concentration of DPPC is too low, it is not adsorbed or coated on the PEEK surface, and no DPPC phospholipid lubrication film is formed [57]. However, as the DPPC concentration increased, the wear rate of PEEK decreased gradually, indicating that DPPC formed a phospholipid lubrication film on the PEEK surface, thereby reducing PEEK wear [29, 36].

4.2 Molecular dynamics simulation

Molecular dynamics (MD) simulation technology uses computers to simulate the movement of molecules and atoms [58] and describe the force motion between particles and the bonding reaction between various particles [59].This paper uses the commercial software Materials Studio to build a three-layer model of β-Si_3N_4 (100) [58], a DPPC aqueous solution, and PEEK. The density of DPPC aqueous solution is set as 1 g/cm^3, (i.e., one DPPC molecule and 246 H_2O molecules) [60, 61]. Because PEEK is a polymer model, the degree of polymerization of the PEEK model is 3–5 and the molecular chain is condensed [62, 63], thus, the equilibrated PEEK chain had a density of 1.35 g/cm^3, which matches the experimental value (1.3 g/cm^3). As shown in Fig. 9, the layers were "sandwiched" and the universal force field was applied. To minimize calculation time and enhance efficiency, the scale of the molecular friction model box was set at 3.1 nm × 2.0 nm × 3.8 nm.

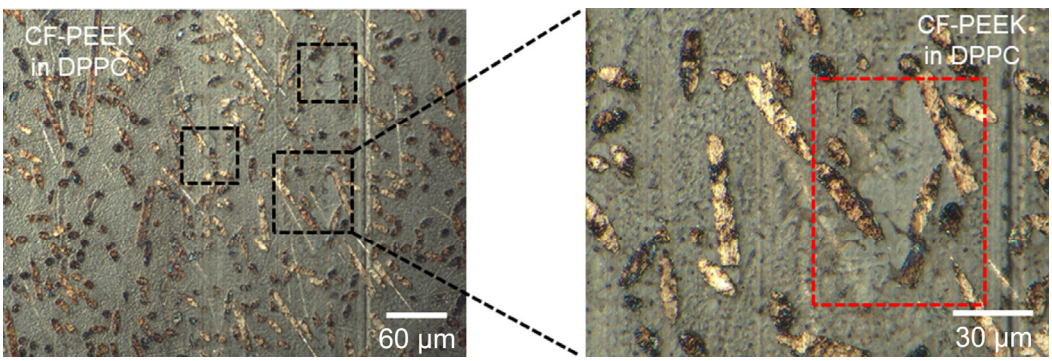

Fig. 7 Microscopy images showing the surface morphology of CF-PEEK in DPPC (1 g/L).

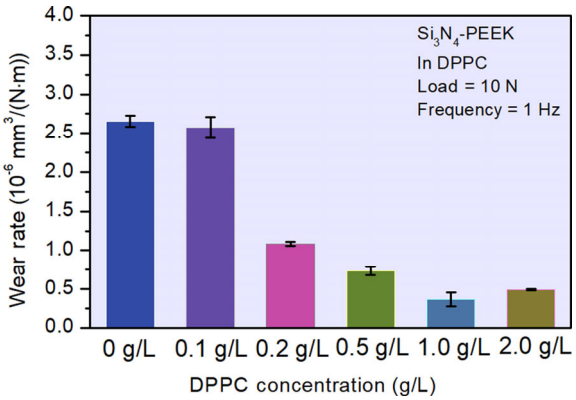

Fig. 8 Wear rates of Si_3N_4/PEEK under different DPPC concentrations (0.1, 0.2, 0.5, 1.0, and 2.0 g/L).

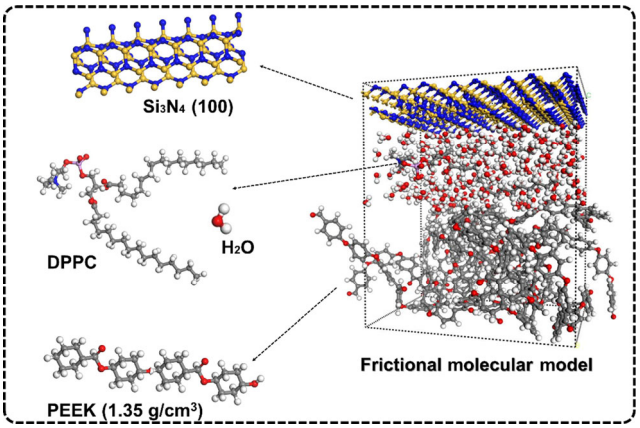

Fig. 9 Si_3N_4/PEEK molecular friction model under DPPC lubrication.

For the calculation, Nosé-Hoover thermostat controls were used to maintain a temperature of 298 K [64], and a canonical NVT (number of particles, volume, temperature) ensemble was applied [65]. A frictional molecular model was used to control the simulation environment of the whole simulation system by using the open-source molecular simulation software LAMMPS. The velocity Verlet algorithm was used to integrate the position and velocity sets [66]. The time step was set to 1 fs and the total time was set to 600 ps. In the simulation system, periodic boundary conditions were used in both X and Y directions. To calculate the total force between materials, images were captured every 20 fs. The long-range interaction was calculated by a particle mesh solver [67]. The cut-off distance of the Lennard–Jones Coulombic interaction was 12 Å.

In the MD simulation, the friction process of Si_3N_4 and PEEK was realized by using the two-process Friction command in the open-source molecular simulation software LAMMPS to account for extrusion in the z-axis negative direction and shearing in the x-axis direction. The positive pressure applied in the z-axis direction was 3 nN. To calculate the friction stability process of Si_3N_4/PEEK under DPPC lubrication the total time was set at 25 ps, and the time step at 5 ps. The friction mechanism of Si_3N_4 and PEEK under DPPC lubrication was analyzed based on the visualized

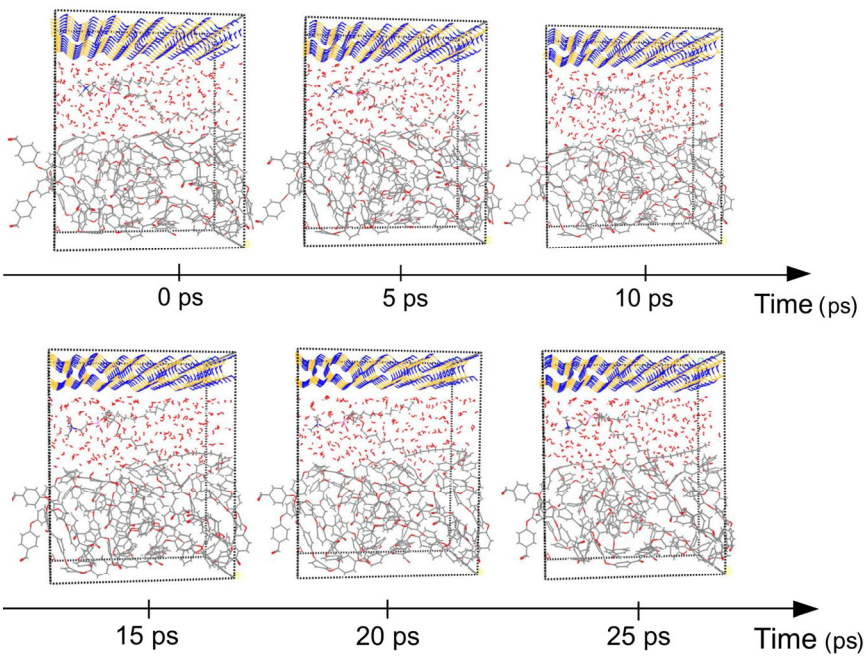

Fig. 10 Line–Stick models of the structural changes of Si_3N_4 and PEEK under DPPC lubrication at 0, 5, 10, 15, 20, and 25 ps.

output of molecular friction model of Si_3N_4 and PEEK under DPPC lubrication. Figure 10 depicts line-stick models of the structural changes of Si_3N_4 and PEEK under DPPC lubrication at 0, 5, 10, 15, 20, and 25 ps.

Figure 11 shows the friction coefficient of Si_3N_4 and PEEK under DPPC lubrication during the period of 0–25 ps, when the friction coefficient remains between 0.06–0.07. The friction coefficient simulated by LAMMPS is consistent with the experimental friction coefficient, which implies that the established model is reasonable. At 0 ps, Si_3N_4, PEEK, and DPPC lubrication were completely distinctive layers. At 10 ps, the water molecules in the DPPC aqueous solution began to diffuse into the PEEK structure, the DPPC molecules were gradually approaching the PEEK chains, and a molecular chain of DPPC had contacted the PEEK layer. That quickly, the DPPC molecules are already beginning to be entangled with the PEEK layer. Note that the friction coefficient of an MD simulation is slightly different from that of actual friction process because the pressure applied in the *z*-axis direction is limited by the molecular model and will be somewhat different from the actual pressure. On the other hand, the concentration of DPPC in aqueous solution is different from that in actual friction. Therefore, it is very reasonable to use LAMMPS program command for Si_3N_4 and PEEK under DPPC aqueous solution.

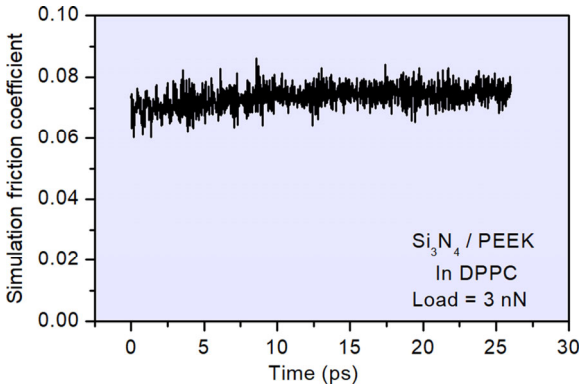

Fig. 11 Simulation friction coefficient of Si_3N_4/PEEK under DPPC lubrication.

4.3 Mechanism discussion

Figure 12 shows the mechanisms by which DPPC lubrication affects the tribological properties of PEEK and CF-PEEK. During tribological testing, small fragments of the DPPC phospholipid in solution will self-assemble to form a large, continuous DPPC phospholipid film on the PEEK surface (Fig. 12(a)) [28, 29]. The phospholipid film coated on the PEEK surface is relatively complete and can withstand the pressure generated by the friction process [68], thereby

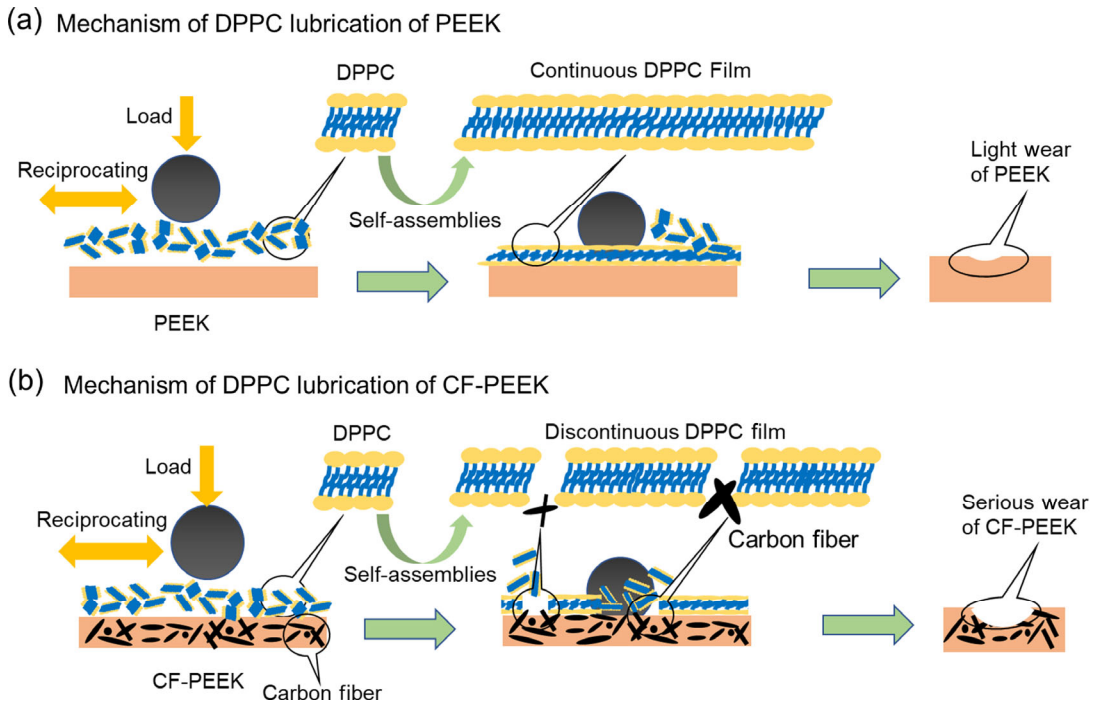

Fig. 12 Schematics showing how the tribological properties of (a) PEEK and (b) CF-PEEK are affected by DPPC lubrication.

protecting the PEEK surface and improving the tribological properties of PEEK. Similarly, for CF-PEEK, the small DPPC fragments in solution self-assemble to form the DPPC phospholipid film [28, 29]; however, due to the presence of carbon fiber ends or the carbon fiber itself, the DPPC phospholipid film is discontinuous and incomplete on the CF-PEEK surface (Fig. 12(b)). The carbon fiber prevents the self-assembly of the DPPC film on the CF-PEEK surface, resulting in a significantly higher wear rate of CF-PEEK compared to PEEK. But and both PEEK and CF-PEEK achieved lower friction coefficient with DPPC (1 g/L) through friction tests. This result may be because DPPC can reduce the friction coefficient by forming a lubricating film on the surface of PEEK and CF-PEEK. DPPC film on surface of CF-PEEK may play a role in establishing a positive pressure-bearing capacity to achieve lower friction coefficient.

5 Conclusions

This study revealed that the presence of carbon fiber in CF-PEEK affects the formation of the phospholipid protective film under DPPC lubrication, causing the wear rate of CF-PEEK to be higher than that of PEEK. Based on our experimental and modeling results, the following conclusions can be drawn:

1) Under water lubrication, the wear rate of CF-PEEK is lower than pure PEEK in contact with different materials (stainless steel, Si_3N_4, Al_2O_3, and ZrO_2), such that the wear rate of CF-PEEK was 50% that of PEEK. For the friction pairs containing stainless steel, the wear rate of CF-PEEK was only 10% that of PEEK. In contrast, under DPPC lubrication, the wear rates of PEEK are 35%–80% lower than the wear rates of CF-PEEK.

2) For the PEEK/Si_3N_4 friction pairs under water lubrication, the CF-PEEK had a lower wear rate than PEEK under all loads (5, 10, and 15 N) and speeds (1, 1.5, and 2 Hz). However, under DPPC lubrication, the wear rates of PEEK are 50%–75% lower than the wear rates of CF-PEEK.

3) During DPPC lubrication, the DPPC self-assembled to form phospholipid films on the PEEK surfaces, inhibiting the wear of PEEK. However, the presence of carbon fiber hindered the self-assembly process of DPPC on the surface of CF-PEEK, preventing the DPPC from forming a continuous phospholipid film. This explains the higher wear rate of CF-PEEK compared to PEEK under DPPC lubrication. In the absence of carbon fiber, a continuous phospholipid film formed on the surface of PEEK, resulting in better wear resistance compared to CF-PEEK.

Acknowledgements

This work was financially supported by the National Natural Science Foundation of China (Grant Nos. 52175180, 51805366) and the Natural Science Foundation of Tianjin City (Grant No. 19JCQNJC04100).

References

[1] Zhao W T, Michalik D, Ferguson S, Hofstetter W, Lemaître J, von Rechenberg B, Bowen P. Rapid evaluation of bioactive Ti-based surfaces using an *in vitro* titration method. *Nat Commun* **10**(1): 2062 (2019)

[2] Blendinger F, Seitz D, Ottenschläger A, Fleischer M, Bucher V. Atomic layer deposition of bioactive TiO_2 thin films on polyetheretherketone for orthopedic implants. *ACS Appl Mater Interfaces* **13**(3): 3536–3546 (2021)

[3] Friedrich K, Chang L, Haupert F. Current and future applications of polymer composites in the field of tribology. In *Composite materials*. Nicolais L, Meo M, Milella E, Ed. London: Springer, 2011: 507–514.

[4] Sikder P, Grice C R, Lin B, Goel V K, Bhaduri S B. Single-phase, antibacterial trimagnesium phosphate hydrate coatings on polyetheretherketone (PEEK) implants by rapid microwave irradiation technique. *ACS Biomater Sci Eng* **4**(8): 2767–2783 (2018)

[5] Brockett C L, Carbone S, Fisher J, Jennings L M. PEEK and CFR-PEEK as alternative bearing materials to UHMWPE in a fixed bearing total knee replacement: An experimental wear study. *Wear* **374–375**: 86–91 (2017)

[6] Song J, Xiang D, Wang S, Liao Z, Lu J, Liu Y, Liu W, Peng Z. *In vitro* wear study of PEEK and CFRPEEK against UHMWPE for artificial cervical disc application. *Tribol Int* **122**: 218–227 (2018)

[7] Steven M K, John N D. PEEK biomaterials in trauma, orthopedic, and spinal implants. *Biomater* **28**(32): 4845–4869 (2007)

[8] Barkarmo S, Wennerberg A, Hoffman M, Kjellin P, Breding K, Handa P, Stenport V. Nano-hydroxyapatite-coated PEEK implants: A pilot study in rabbit bone. *J Biomed Mater Res Part A* **101**(2): 465–471 (2012)

[9] Raj A, Wang M, Zander T, Wieland D C F, Liu X, An J, Garamus V M, Mer R W R, Fielden M, Claesson P M. Lubrication synergy: Mixture of hyaluronan and dipalmitoyl phosphatidylcholine (DPPC) vesicles. *J Colloid Interf Sci* **488**: 225–333 (2017)

[10] Jin Z M, Dowson D. Bio-friction. *Friction* **1**(2): 100–113 (2013)

[11] Hassan E A M, Ge D, Yang L, Zhou J, Liu M, Yu M, Zhu S. Highly boosting the interlaminar shear strength of CF/PEEK composites via introduction of PEKK onto activated CF. *Composites Part A* **112**: 155–160 (2018)

[12] Wang X, Huang Z, Lai M, Jiang L, Zhang Y, Zhou H. Highly enhancing the interfacial strength of CF/PEEK composites by introducing PAIK onto diazonium functionalized carbon fibers. *Appl Surf Sci* **510**: 145400 (2020)

[13] Yan M, Tian X, Peng G, Li D, Zhang X. High temperature rheological behavior and sintering kinetics of CF/PEEK composites during selective laser sintering. *Compos Sci Technol* **165**: 140–147 (2018)

[14] Maharaj G, Bleser S, Albert K, Lambert R, Jani S, Jamison R. Characterization of wear in composite material orthopaedic implants part I: The composite trunnion/ceramic head interface. *Bio-Med Mater Eng* **4**(3): 193–198 (1994)

[15] Wang A, Lin R, Polineni V K, Essner A, Stark C, Dumbleton J H. Carbon fiber reinforced polyether ether ketone composite as a bearing surface for total hip replacement. *Tribol Int* **31**(11): 661–667 (1998)

[16] Mankin H J. The response of articular cartilage to mechanical injury. *J Bone Joint Surg* **64**(3): 460–466 (1982)

[17] Fam H, Kontopoulou M, Bryant J T. Effect of concentration and molecular weight on the rheology of hyaluronic acid/bovine calf serum solutions. *Biorheology* **46**: 31–43 (2009)

[18] Brandt J M, Brière L K, Marr J, MacDonald S J, Bourne R B, Medley J B. Biochemical comparisons of osteoarthritic human synovial fluid with calf sera used in knee simulator wear testing. *J Biomed Mater Res Part A* **94A**(3): 961–971 (2010)

[19] Liu H T, Ge S R, Cao S F, Wang S B. Comparison of wear debris generated from ultra high molecular weight polyethylene in vivo and in artificial joint simulator. *Wear* **271**(5): 647–652 (2011)

[20] Xin H, Liu R, Zhang L, Jia J H, Jin Z M. A comparative bio-tribological study of self-mated PEEK and its composites under bovine serum lubrication. *Biotribology* **26**: 100171 (2021)

[21] R Gale L, Chen Y, A Hills B, Crawford R. Boundary lubrication of joints: Characterization of surface-active phospholipids found on retrieved implants. *Acta Orthop* **78**(3): 309–314 (2007)

[22] Csanádi T, Gall M, Vojtko M, Kovalčíková A, Hnatko M, Dusza J, Šajgalík, P. Micro scale fracture strength of grains and grain boundaries in polycrystalline La-doped β-Si_3N_4 ceramics. *J Eur Ceram Soc* **40**(14): 4783–4791 (2020)

[23] Wang H D, Liu Y H, Zhao J, Li J J, Wang Q, Luo J B. Tribological behavior of layered double hydroxides with various chemical compositions and morphologies as grease additives. *Friction* **9**(5): 952–962 (2021)

[24] Andrieux K, Forte L, Lesieur S, Paternostre M, Ollivon M, Grabielle-Madelmont C. Solubilisation of dipalmitoylphosphatidylcholine bilayers by sodium taurocholate: A model to study the stability of liposomes in the gastrointestinal tract and their mechanism of interaction with a model bile salt. *Eur J Pharm Biopharm* **71**(2): 346–355 (2009)

[25] Li J, Wang X, Zhang T, Wang C, Huang Z, Luo X, Deng Y. A review on phospholipids and their main applications in drug delivery systems. *Asian J Pharm Sci* **10**(2): 81–98 (2015)

[26] Jahn S, Klein J. Lubrication of articular cartilage. *Phys Today* **71**(4): 48–54 (2018)

[27] Klein J. Repair or replacement—A joint perspective. *Science* **323**(5910): 47 (2009)

[28] Sorkin R, Kampf N, Zhu L, Klein J. Hydration lubrication and shear-induced self-healing of lipid bilayer boundary lubricants in phosphatidylcholine dispersions. *Soft Matter* **12**(10): 2773–2784 (2016)

[29] Angayarkanni S A, Kampf N, Klein J. Lipid-bilayer assemblies on polymer-bearing surfaces: The nature of the

slip plane in asymmetric boundary lubrication. *Langmuir* **36**(51): 15583–15591 (2020)

[30] Pezzotti G, Yamamoto K. Artificial hip joints: The biomaterials challenge. *J Mech Behav Biomed Mater* **31**: 3–20 (2014)

[31] McEntire B J, Bal B S, Rahaman M N, Chevalier J, Pezzotti G. Ceramics and ceramic coatings in orthopaedics. *J Eur Cera Soc* **35**(16): 4327–4369 (2015)

[32] Oner F K, Alakent B, Soyer-Uzun S. Effect of silane A-174 modifications in the structure, chemistry, and compressive strength of PLA-HAP and PLA-β-TCP biocomposites: Toward the design of polymer–ceramic implants with high performance. *ACS Appl Polym Mater* **3**(5): 2432–2446 (2021)

[33] Böke F, Giner I, Keller A, Grundmeier G, Fischer H. Plasma-enhanced chemical vapor deposition (PE-CVD) yields better hydrolytical stability of biocompatible siox thin films on implant alumina ceramics compared to rapid thermal evaporation physical vapor deposition (PVD). *ACS Appl Mater Interfaces* **8**(28): 17805–17816 (2016)

[34] Wang Z, Li J, Ge X, Liu Y, Luo J, Chetwynd D G, Mao K. Investigation of the lubrication properties and synergistic interaction of biocompatible liposome-polymer complexes applicable to artificial joints. *Colloids Surf B* **178**: 469–478 (2019)

[35] East R H, Briscoe A, Unsworth A. Wear of PEEK-OPTIMA® and PEEK-OPTIMA®-wear performance articulating against highly cross-linked polyethylene. *J Eng Med* **229**(3): 187–193 (2015)

[36] Goldberg R, Schroeder A, Silbert G, Turjeman K, Barenholz Y, Klein J. Boundary lubricants with exceptionally low friction coefficients based on 2D close-packed phosphatidylcholine liposomes. *Adv Mater* **23**(31): 3517–3521 (2011)

[37] Raviv U, Klein J. Fluidity of bound hydration layers. *Science* **297**(5586): 1540–1543 (2002)

[38] Chen M, Briscoe W H, Armes S P, Klein J. Lubrication at physiological pressures by polyzwitterionic brushes. *Science* **323**(5922): 1698–1701 (2009)

[39] Briscoe W H, Titmuss S, Tiberg F, Thomas R K, McGillivray D J, Klein J. Boundary lubrication under water. *Nature* **444**(7116): 191–194 (2006)

[40] Lin W F, Kluzek M, Iuster N, Shimoni E, Kampf N, Goldberg R, Klein J. Cartilage-inspired, lipid-based boundary-lubricated hydrogels. *Science* **370**(6514): 335–338 (2020)

[41] Blau P J. Lessons learned from the test-to-test variability of different types of wear data. *Wear* **376–377**: 1830–1840 (2017)

[42] Bal B S, Rahaman M N. Orthopedic applications of silicon nitride ceramics. *Acta Biomater* **8**(8): 2889–2898 (2012)

[43] Li C S, Vannabouathong C, Sprague S, Bhandari M. The use of carbon-fiber-reinforced (CFR) PEEK material in orthopedic implants: A systematic review. *Clin Med Insights: Arthritis Musculoskeletal Disord* **8**: 33–45 (2015)

[44] Sakka M M, Antar Z, Elleuch K, Feller J F. Tribological response of an epoxy matrix filled with graphite and/or carbon nanotubes. *Friction* **5**(2): 171–182 (2017)

[45] Raviv U, Giasson S, Kampf N, Gohy J F, Jéröme R, Klein J. Lubrication by charged polymers. *Nature* **425**(6954): 163–165 (2003)

[46] Braun D, Greiner C, Schneider J, Gumbsch P. Efficiency of laser surface texturing in the reduction of friction under mixed lubrication. *Tribol Int* **77**: 142–147 (2014)

[47] Zhu J, Ma L, Dwyer-Joyce R. Friction and wear behaviours of self-lubricating peek composites for articulating pin joints. *Tribol Int* **149**: 105741 (2020)

[48] Wang A, Lin R, Stark C, Dumbleton J H. Suitability and limitations of carbon fiber reinforced PEEK composites as bearing surfaces for total joint replacements. *Wear* **225–229**(2): 724–727 (1999)

[49] Regis M, Lanzutti A, Bracco P, Fedrizzi L. Wear behavior of medical grade PEEK and CFR PEEK under dry and bovine serum conditions. *Wear* **408–409**: 86–95 (2018)

[50] Borruto A. A new material for hip prosthesis without considerable debris release. *Med Eng Phy* **32**(8): 908–913 (2010)

[51] Yamamoto Y, Hashimoto M. Friction and wear of water lubricated PEEK and PPS sliding contacts. *Wear* **257**(1–2): 181–189 (2004)

[52] Goldberg R, Klein J. Liposomes as lubricants: beyond drug delivery. *Chem Phys Lipids* **165**(4): 374–381 (2012)

[53] Cao Y, Kampf N, Kosinska M K, Steinmeyer J, Klein J. Interactions between bilayers of phospholipids extracted from human osteoarthritic synovial fluid. *Biotribology* **25**: 100157 (2021)

[54] Lin W, Mashiah R, Seror J, Kadar A, Dolkart O. Lipid-hyaluronan synergy strongly reduces intrasynovial tissue boundary friction. *Acta Biomate* **83**: 314–321 (2019)

[55] Sorkin R, Dror Y, Kampf N, Klein J. Mechanical stability and lubrication by phosphatidylcholine boundary layers in the vesicular and in the extended lamellar phases. *Langmuir* **30**(17): 5005–5014 (2014)

[56] Lin W, Kluzek M, Iuster N, Shimoni E, Klein J. Cartilage-inspired, lipid-based boundary-lubricated hydrogels. *Science* **370**(6514): 335–338 (2020)

[57] Lin W, Liu Z, Kampf N, Klein J. The role of hyaluronic acid in cartilage boundary lubrication. *Cells* **9**(7): 1606 (2020)

[58] Shargh A K, Abdolrahim N. Molecular dynamics simulation

of structural changes in single crystalline silicon nitride nanomembrane. *Ceram Int* **45**(17B): 23070–23077 (2019)

[59] Yao J, Wu Y, Sun J, Xu Y, Wang H, Zhou P. Research on the metamorphic layer of silicon nitride ceramic under high temperature based on molecular dynamics. *Int J Adv Manuf Technol* **109**(5): 1249–1260 (2020)

[60] Shinoda W, DeVane R, Klein M L. Zwitterionic lipid assemblies: Molecular dynamics studies of monolayers, bilayers, and vesicles using a new coarse grain force field. *J Phys Chem B* **114**(20): 6836–6849 (2010)

[61] Mohammed L, Nourddine H, Saad E F, Abdelali D, Hamid R. Chitosan-covered liposomes as a promising drug transporter: nanoscale investigations. *RSC Adv* **11**(3): 1503–1516 (2021)

[62] Tsafack T, Bartolucci S F, Maurer JA . An atomistic view of heat propagation from graphene to polyether ether ketone (PEEK). *Comput Mater Sci* **177**: 109590 (2020)

[63] Jung H, Bae K J, Jin J U, Oh Y, Hong H, Youn S J, You N H, Yu J. The effect of aqueous polyimide sizing agent on PEEK based carbon fiber composites using experimental techniques and molecular dynamics simulations. *Funct Compos Struct* **2**(2): 025001 (2020)

[64] Glasser A H, Sovinec C R, Nebel R A, Gianakon T A, Plimpton S J, Chu M S, Schnack D D. The NIMROD code: A new approach to numerical plasma physics. *Plasma Phys Controlled Fusion* **41**(3A): A747–A755 (1999)

[65] Labík S, Smith W R. Scaled particle theory and the efficient calculation of the chemical potential of hard spheres in the NVT ensemble. *Mol Sim* **12**(1): 23–31 (1994)

[66] Martys N S, Mountain R D. Velocity Verlet algorithm for dissipative-particle-dynamics-based models of suspensions. *Physi Rev E* **59**(3): 3733–3736 (1999)

[67] Beckers J V L, Lowe C P, De Leeuw S W. An iterative PPPM method for simulating coulombic systems on distributed memory parallel computers. *Mol Sim* **20**(6): 369–383 (1998)

[68] Zhu L, Seror J, Day A J, Kampf N, Klein J. Ultra-low friction between boundary layers of hyaluronan-phosphatidylcholine complexes. *Acta Biomater* **59**: 283–292 (2017)

Shuai YAN. He received his M.S. and Ph.D. degrees from Tianjin University in 2010 and 2015, respectively. He is an associate professor at the Key Laboratory of Advanced Ceramics and Machining Technology of Ministry of Education of Tianjin University. He was selected as "Peiyang Scholar-Young Backbone Teacher" by Tianjin University. His research interests focus on ceramic tribology and ceramic precision machining.

Shichao MEN. He joined the Key Laboratory of Advanced Ceramics and Machining Technology of Ministry of Education at Tianjin University from 2019. Currently, he has been studying for his M.S. degree in the School of Material Engineering of Tianjin University. His research interests include the tribology of ceramic and polymer orthopaedic implants.

Bin LIN. He is a tenured professor in the School of Mechanical Engineering at Tianjin University. His current identity is a doctoral supervisor and the vice-director of the Key Laboratory of Advanced Ceramics and Machining Technology of Ministry of Education. His research areas cover machining theory and technology of hard and brittle materials, and application technology of hard and brittle materials.